mathematics

Article

The Improvement of the Discrete Wavelet Transform

Zhihua Zhang

School of Mathematics, Shandong University, Jinan 250100, China; zhangzhihua@sdu.edu.cn

Abstract: Discrete wavelet transforms are widely used in signal processing, data compression and spectral analysis. For discrete data with finite sizes, one always pads the data with zeros or extends the data into periodic data before performing the discrete periodic wavelet transform. Due to discontinuity on the boundaries of the original data, the obtained wavelet coefficients always decay slowly, leading to data compression ratios that are significantly lower. In order to solve this issue, in this study, we coupled polynomial fitting into classic discrete periodic wavelet transforms to mitigate these boundary effects.

Keywords: discrete wavelet transform; boundary effects; biorthonomal periodic wavelet; fast algorithm

MSC: 42C

check for updates

Citation: Zhang, Z. The Improvement of the Discrete Wavelet Transform. *Mathematics* **2023**, *11*, 1770. https://doi.org/10.3390/math11081770

Academic Editor: Vladimir Balan

Received: 16 March 2023
Revised: 30 March 2023
Accepted: 3 April 2023
Published: 7 April 2023

1. Introduction

The application of wavelets in data compression, denoising and time-frequency representation [1–6] requires that the wavelets are real-valued, (anti)symmetric and compactly supported. Classic orthogonal wavelets cannot achieve these properties, so the orthogonality in wavelets is relaxed to biorthogonality [7–12]. Let $\psi(t)$ and $\widetilde{\psi}(t)$ be a pair of real-valued compactly supported biorthonomal wavelets in $L^2(\mathbb{R})$ that are generated by real-valued compactly supported scaling functions $\varphi(t)$ and $\widetilde{\varphi}(t)$. The frequently used wavelets in higher dimensions just consist of tensor products of one-dimensional wavelets, e.g., we can generate the tensor product of $\varphi(t)$ and $\psi(t)$ as follows:

$$\varphi_0(t_1,t_2) = \varphi(t_1)\varphi(t_2), \qquad \psi_1(t_1,t_2) = \varphi(t_1)\psi(t_2),$$

$$\psi_2(t_1,t_2) = \psi(t_1)\varphi(t_2), \qquad \psi_3(t_1,t_2) = \psi(t_1)\psi(t_2).$$

Similarly, taking the tensor products of $\widetilde{\varphi}(t)$ and $\widetilde{\psi}(t)$, we can obtain $\widetilde{\varphi}(t_1,t_2)$, $\widetilde{\psi}_1(t_1,t_2)$, $\widetilde{\psi}_2(t_1,t_2)$ and $\widetilde{\psi}_3(t_1,t_2)$. Then, $\{\psi_\mu(t_1,t_2)\}_{\mu=1,2,3}$ and $\{\widetilde{\psi}_\mu(t_1,t_2)\}_{\mu=1,2,3}$ are a pair of two-dimensional biorthonomal wavelets of $L^2(\mathbb{R}^2)$.

Denote

$$\psi_{\mu,m,\mathbf{n}}(\mathbf{t}) =: 2^m\psi_\mu(2^m\mathbf{t}-\mathbf{n}) = 2^m\psi_\mu(2^m t_1 - n_1, 2^m t_2 - n_2) \qquad (\mathbf{t}=(t_1,t_2),\ \mathbf{n}=(n_1,n_2)).$$

Any function $f \in C^l(\mathbb{R}^2)$ can be expanded into a biorthonomal wavelet series:

$$f(\mathbf{t}) = \sum_{\mathbf{n}} c^w_{m,\mathbf{n}}\widetilde{\varphi}_{0,m,\mathbf{n}}(\mathbf{t}) + \sum_{\mu=1}^{3}\sum_{m=0}^{+\infty}\sum_{\mathbf{n}} d^w_{\mu,m,\mathbf{n}}\widetilde{\psi}_{\mu,m,\mathbf{n}}(\mathbf{t}),$$

where

$$c^w_{m,\mathbf{n}} = \int_{\mathbb{R}}\int_{\mathbb{R}} f(\mathbf{t})\overline{\varphi}_{0,m,\mathbf{n}}(\mathbf{t})\,d\mathbf{t}, \qquad d^w_{\mu,m,\mathbf{n}} = \int_{\mathbb{R}}\int_{\mathbb{R}} f(\mathbf{t})\overline{\psi}_{\mu,m,\mathbf{n}}(\mathbf{t})\,d\mathbf{t}.$$

If $\varphi, \widetilde{\varphi}, \psi, \widetilde{\psi} \in C^l(\mathbb{R})$, then wavelet coefficients of any smooth function $f \in C^l(\mathbb{R}^2)$ satisfy [1,2]

$$d^w_{\mu,m,\mathbf{n}} = O(2^{-m(l+1)}). \tag{1}$$

The associated wavelet filter banks $\{h_k\}$ and $\{\tau_k\}$ are

$$h_k = \sqrt{2}\int_{\mathbb{R}} \varphi(t)\widetilde{\varphi}(2t-k)dt,$$

$$\tau_k = \sqrt{2}\int_{\mathbb{R}} \psi(t)\widetilde{\varphi}(2t-k)dt.$$

Then, the one-dimensional wavelet coefficients satisfy the following:

$$\begin{aligned} c^w_{m-1,k} &= \sum_n h_{n-2k} c^w_{m,n}, \\ d^w_{m-1,k} &= \sum_n \tau_{n-2k} c^w_{m,n}, \end{aligned} \tag{2}$$

and the two-dimensional wavelet coefficients satisfy

$$\begin{aligned} c^w_{m-1,k_1,k_2} &= \sum_{n_1,n_2} h_{n_1-2k_1}\ h_{n_2-2k_2} c^w_{m,n_1,n_2}, \\ d^w_{1,m-1,k_1,k_2} &= \sum_{n_1,n_2} h_{n_1-2k_1}\ \tau_{n_2-2k_2} c^w_{m,n_1,n_2}, \\ d^w_{2,m-1,k_1,k_2} &= \sum_{n_1,n_2} \tau_{n_1-2k_1}\ h_{n_2-2k_2} c^w_{m,n_1,n_2}, \\ d^w_{3,m-1,k_1,k_2} &= \sum_{n_1,n_2} \tau_{n_1-2k_1}\ \tau_{n_2-2k_2} c^w_{m,n_1,n_2}, \end{aligned} \tag{3}$$

see [1]. Formulas (2) and (3) are the one-dimensional and two-dimensional *discrete wavelet transforms* (DWTs), respectively [1,2].

Biorthonomal wavelets can be extended to deal with periodic data. The periodization of any function $h(\mathbf{t})$ is denoted by

$$h^{per}(\mathbf{t}) =: \sum_{\mathbf{k}\in\mathbb{Z}^2} h(\mathbf{t}+\mathbf{k}).$$

The families generated by the periodization of φ, ψ, $\widetilde{\varphi}$ and $\widetilde{\psi}$, namely

$$\psi^{per} = \{\varphi_0^{per}\} \bigcup \{\psi^{per}_{\mu,m,\mathbf{n}},\ \mu = 1,2,3,\ m = 0,1,2,\ldots,\ n_1,n_2 = 0,1,\ldots,2^m-1\},$$

$$\widetilde{\psi}^{per} = \{\widetilde{\varphi}_0^{per}\} \bigcup \{\widetilde{\psi}^{per}_{\mu,m,\mathbf{n}},\ \mu = 1,2,3,\ m = 0,1,2,\ldots,\ n_1,n_2 = 0,1,\ldots,2^m-1\},$$

are a pair of biorthonomal periodic wavelet bases for $L^2([-\frac{1}{2},\frac{1}{2}]^2)$ [1,2]. Any periodic function $f \in C^l([-\frac{1}{2},\frac{1}{2}]^2)$ can be expanded into a biorthonomal periodic wavelet series:

$$f(\mathbf{t}) = c_{0,\mathbf{0}} + \sum_{\mu=1}^{3}\sum_{m=0}^{\infty}\sum_{n_1,n_2=0}^{2^m-1} d_{\mu,m,\mathbf{n}} \widetilde{\psi}^{per}_{\mu,m,\mathbf{n}}(\mathbf{t}),$$

where

$$c_{m,\mathbf{n}} = \int_{-\frac{1}{2}}^{\frac{1}{2}}\int_{-\frac{1}{2}}^{\frac{1}{2}} f(\mathbf{t})\overline{\varphi}^{per}_{0,m,\mathbf{n}}(\mathbf{t})\,d\mathbf{t}, \qquad d_{\mu,m,\mathbf{n}} = \int_{-\frac{1}{2}}^{\frac{1}{2}}\int_{-\frac{1}{2}}^{\frac{1}{2}} f(\mathbf{t})\overline{\psi}^{per}_{\mu,m,\mathbf{n}}(\mathbf{t})\,d\mathbf{t}.$$

If $\varphi, \widetilde{\varphi}, \psi, \widetilde{\psi} \in C^l(\mathbb{R})$, then periodic wavelet coefficients of any smooth periodic function $f \in C^l([-\frac{1}{2},\frac{1}{2}]^2) \bigcap C^l(\mathbb{R}^2)$ satisfy

$$d_{\mu,m,\mathbf{n}} = O(2^{-m(l+1)}). \tag{4}$$

Noticing that $\varphi(t)$ and $\widetilde{\varphi}(t)$ are compactly supported, there exists a positive integer N such that

$$h_k = \tau_k = 0 \qquad (|k| \geq N).$$

We take $2^{m_0-1} > N$ and then define $2^{m_0}-$periodic sequences $\{h_n^*\}$ and $\{\tau_n^*\}$ such that

$$\begin{aligned} h_k^* &= h_k, & \tau_k^* &= \tau_k & & (|k| \leq 2^{m_0-1}), \\ h_{k+2^{m_0}}^* &= h_k^*, & \tau_{k+2^{m_0}}^* &= \tau_k^* & & (k \in \mathbb{Z}). \end{aligned}$$

For $m \geq m_0$, the one-dimensional periodic wavelet coefficients satisfy the following:

$$\begin{aligned} c_{m-1,k} &= \sum_{n=0}^{2^m-1} h_{n-2k}^* c_{m,n}, \\ d_{m-1,k} &= \sum_{n=0}^{2^m-1} \tau_{n-2k}^* c_{m,n}, \end{aligned} \tag{5}$$

and the two-dimensional periodic wavelet coefficients satisfy

$$\begin{aligned} c_{m-1,k_1,k_2} &= \sum_{n_1,n_2=0}^{2^m-1} h_{n_1-2k_1}^* \; h_{n_2-2k_2}^* c_{m,n_1,n_2}, \\ d_{1,m-1,k_1,k_2} &= \sum_{n_1,n_2=0}^{2^m-1} h_{n_1-2k_1}^* \; \tau_{n_2-2k_2}^* c_{m,n_1,n_2}, \\ d_{2,m-1,k_1,k_2} &= \sum_{n_1,n_2=0}^{2^m-1} \tau_{n_1-2k_1}^* \; h_{n_2-2k_2}^* c_{m,n_1,n_2}, \\ d_{3,m-1,k_1,k_2} &= \sum_{n_1,n_2=0}^{2^m-1} \tau_{n_1-2k_1}^* \; \tau_{n_2-2k_2}^* c_{m,n_1,n_2}, \end{aligned} \tag{6}$$

see [1]. Formulas (5) and (6) are one-dimensional and two-dimensional *discrete periodic wavelet transforms* (DPWTs), respectively [1,2]. Since the convolution of finite length data are always computed approximately by circular convolution in signal processing and data analysis, there is no big difference between (2) and (3) and (5) and (6); hence, the DPWT is considered to be the same as the DWT.

The DWT/DPWT has become a routine fast algorithm in various signal processing fields such as data compression, spectral analysis, denoising, mechanical fault diagnosis, etc. Zeng [13] used two-dimensional DWTs to extract weak information from the gamma spectrum; Alaifari et al. [14] developed a recovery algorithm of square-integrable signals from the absolute values of their wavelet transforms; Lin [15] applied the DWT to the simulation of corrosion fields on buried pipelines; Torrence and Compo [15] developed an empirical formula for the statistical significance testing of DWTs of signals against red noise. Later on, Zhang [16] extended this empirical formula to the generalized case and gave the proof in the rigid statistical framework. Since all data used in this research are of a finite size, we always needed to either pad the data with zeros before performing the DWT or extend the data into periodic data before performing the DPWT. Due to discontinuity on the data boundary, the associated wavelet coefficients always decayed slowly, leading to data compression ratios that were significantly lower and wavelet spectra that were distorted. Although the DWT/DPWT has been widely used in different fields (e.g., [13–18]), until now there has been no method to delete or mitigate boundary effects in the DWT/DPWT.

In this study, we coupled simple polynomial fitting with a classic DWT/DPWT to mitigate boundary effects on wavelet coefficients. In Section 2, since our proposed algorithm is complex, we first briefly introduce the simplest version of our improved DWT/DPWT algorithm and show how boundary discontinuities are mitigated in our improvement. In Section 3, we discuss the continuous version of our improvement and show the advantages of our improvement. In Section 4, we establish, step by step, a full version of our improvement of the DWT/DPWT. In Section 5, we give details of some numerical experiments that we used to test our improvement algorithm. In Section 6, we summarize the advantages of our improvement algorithm and discuss some potential applications.

2. Our Improvement of the DWT: The Simplest Version

In order to mitigate boundary effects in DWT/DPWT, we proposed the following algorithm.

First, the discrete data, $\{x_{n_1,n_2}\}_{n_1,n_2=0,1,\dots,2^J-1}$, are decomposed into three parts:

$$x_{n_1,n_2} = y^{(2)}_{n_1,n_2} - y^{(1)}_{n_1,n_2} + z_{n_1,n_2}, \tag{7}$$

where

$$\begin{aligned} y^{(1)}_{n_1,n_2} &= x_{0,0}(1-\tfrac{2n_1}{2^J})(1-\tfrac{2n_2}{2^J}) + x_{0,2^{J-1}}(1-\tfrac{2n_1}{2^J})(\tfrac{2n_2}{2^J}) + x_{2^{J-1},0}(\tfrac{2n_1}{2^J})(1-\tfrac{2n_2}{2^J}) + x_{2^{J-1},2^{J-1}}(\tfrac{2n_1}{2^J})(\tfrac{2n_2}{2^J}), \\ y^{(2)}_{n_1,n_2} &= x_{0,n_2}(1-\tfrac{2n_1}{2^J}) + x_{2^{J-1},n_2}(\tfrac{2n_1}{2^J}) + x_{n_1,0}(1-\tfrac{2n_2}{2^J}) + x_{n_1,2^{J-1}}(\tfrac{2n_2}{2^J}). \end{aligned}$$

The computation of $y^{(1)}_{n_1,n_2}$ depends on the values $\{x_{0,0}\}$, $\{x_{0,2^{J-1}}\}$, $\{x_{2^{J-1},0}\}$ and $\{x_{2^{J-1},2^{J-1}}\}$. The computation of $y^{(2)}_{n_1,n_2}$ depends on the boundary data $\{x_{n_1,0}\}$, $\{x_{n_1,2^{J-1}}\}$, $\{x_{0,n_2}\}$ and $\{x_{2^{J-1},n_2}\}$, which can be further decomposed as follows:

$$\begin{aligned} x_{n_1,0} &= x_{0,0}(1-\tfrac{2n_1}{2^J}) + x_{2^{J-1},0}(\tfrac{2n_1}{2^J}) + w^0_{n_1}, \\ x_{n_1,2^{J-1}} &= x_{0,2^{J-1}}(1-\tfrac{2n_1}{2^J}) + x_{2^{J-1},2^{J-1}}(\tfrac{2n_1}{2^J}) + w^1_{n_1}, \\ x_{0,n_2} &= x_{0,0}(1-\tfrac{2n_2}{2^J}) + x_{0,2^{J-1}}(\tfrac{2n_2}{2^J}) + v^0_{n_2}, \\ x_{2^{J-1},n_2} &= x_{2^{J-1},0}(1-\tfrac{2n_2}{2^J}) + x_{2^{J-1},2^{J-1}}(\tfrac{2n_2}{2^J}) + v^1_{n_2}. \end{aligned} \tag{8}$$

Next, an odd extension, and then a periodic extension, for $\{w^0_{n_1}\}$, $\{w^1_{n_1}\}$, $\{v^0_{n_2}\}$, $\{v^1_{n_2}\}$ and $\{z_{n_1,n_2}\}$ are performed. By (2.1) and (2.2), it is clear that for $n_1 = 0, 2^{J-1}$ or $n_2 = 0, 2^{J-1}$,

$$z_{n_1,n_2} = 0, \qquad w^0_{n_1} = 0, \qquad w^1_{n_1} = 0, \qquad v^0_{n_2} = 0, \qquad v^1_{n_2} = 0,$$

so we can easily deduce that the above odd and periodic extensions guarantee continuity and differentiability on the data boundary. Finally, one-dimensional and two-dimensional DWTs/DPWTs are performed for these extension data.

Due to the smooth extension in our improvement, by (1) and (4), the decay rate of the obtained wavelet coefficients in our improvement algorithm is faster than that of traditional (periodic) wavelet coefficients. This means that our improvement can compress the data better than the traditional DWT/DPWT. Our proposed algorithm can be further modified to achieve higher compression ratios. The full version of our improved algorithm is summarized at the end of Section 4.

3. Continuous Version of Our Improved Wavelet Algorithm

In order to explain the advantages of our improved algorithm over traditional wavelet algorithms, we established a step by step continuous version of our improved wavelet algorithm.

Denote $D^{(\alpha,\beta)}f = \frac{tial^{\alpha+\beta}}{tialt_1^{\alpha}\, tialt_2^{\beta}} f$. If $D^{(\alpha,\beta)}f$ is continuous on the region Ω for all α, $\beta \le l$, we say $f \in C^l(\Omega)$. Let the fundamental polynomial $p_m(t)$ be a univariate polynomial of degree $2m+1$ satisfying

$$D^{(2\lambda)}p_m(0) = 0, \qquad D^{(2\lambda)}p_m(1) = \delta_{\lambda,m}, \tag{9}$$

where $\delta_{\lambda,m} = 0\,(\lambda \neq m)$ and $\delta_{\lambda,m} = 1\,(\lambda = m)$. Then, $p_m(t)$ can be represented as follows:

$$p_m(t) = \frac{1}{(2m+1)!}t^{2m+1} + \sum_{k=0}^{m-1} c_k t^{2k+1},$$

where the coefficients, $\{c_k\}_{k=0,\dots,m-1}$, satisfy

$$\sum_{k=j}^{m-1} \frac{(2k+1)!}{(2k-2j+1)!} c_k = -\frac{1}{(2m-2j+1)!} \qquad (j = 0, 1, \dots, m-1).$$

For any function $f \in C^l([0, \frac{1}{2}])$, define the interpolation polynomial of f at the nodes 0 and $\frac{1}{2}$:

$$h(t) = \sum_{k=0}^{n} \frac{1}{2^{2k}} \left(D^{(2k)} f(0) p_k(1-2t) + D^{(2k)} f\left(\frac{1}{2}\right) p_k(2t) \right) \qquad (0 \le t \le \frac{1}{2}),$$

where $n = [\frac{l}{2}]$ and $[\cdot]$ represent the integral part. Then, $h(t)$ satisfies

$$D^{(2j)} h(0) = D^{(2j)} f(0),\ D^{(2j)} h(\frac{1}{2}) = D^{(2j)} f(\frac{1}{2}) \qquad (j = 0, 1, \dots, n).$$

Let $r(t) = f(t) - h(t)$ $(t \in [0, \frac{1}{2}])$. Then,

$$r^{(2j)}(0) = r^{(2j)}(\frac{1}{2}) = 0\,(j = 0, 1, \dots, n). \tag{10}$$

For $r(t)$, an odd extension is performed, which is denoted by $r^o(t)$. Again, a 1-periodic extension of $r^o(t)$ is performed to obtain $\widetilde{r}(t)$. By (10), it follows that $\widetilde{r} \in C^l(\mathbb{R})$, i.e., the univariate function $f \in C^l([0, \frac{1}{2}])$ can be decomposed as follows:

$$f(t) = h(t) + \widetilde{r}(t),$$

where $h(t)$ is the interpolation polynomial of f at the nodes 0 and $\frac{1}{2}$, $\widetilde{r}(t)$ is a 1-periodic odd function and $\widetilde{r} \in C^l(\mathbb{R})$.

For a bivariate smooth function $f \in C^l([0, \frac{1}{2}]^2)$, denote $\mathbf{t} = (t_1, t_2)$ and $n = \left[\frac{l}{2}\right]$. Define $\tau_1(\mathbf{t})$ as the interpolation polynomial of f at the vertices of $[0, \frac{1}{2}]^2$:

$$\begin{aligned} \tau_1(\mathbf{t}) = \sum_{\alpha,\beta=0}^{n} 2^{-2\alpha-2\beta} [\, & D^{(2\alpha,2\beta)} f(0,0) p_\alpha(1-2t_1) p_\beta(1-2t_2) \\ & + D^{(2\alpha,2\beta)} f(0, \tfrac{1}{2}) p_\alpha(1-2t_1) p_\beta(2t_2) \\ & + D^{(2\alpha,2\beta)} f(\tfrac{1}{2}, 0) p_\alpha(2t_1) p_\beta(1-2t_2) \\ & + D^{(2\alpha,2\beta)} f(\tfrac{1}{2}, \tfrac{1}{2}) p_\alpha(2t_1) p_\beta(2t_2)\,], \end{aligned} \tag{11}$$

such that for $0 \le \alpha, \beta \le n$ and $(t_1, t_2) = (0,0), (0, \frac{1}{2}), (\frac{1}{2}, 0), (\frac{1}{2}, \frac{1}{2})$,

$$D^{(2\alpha,2\beta)} \tau_1(t_1, t_2) = D^{(2\alpha,2\beta)} f(t_1, t_2).$$

Define

$$\begin{aligned} \tau_2(\mathbf{t}) = & \sum_{\alpha=0}^{n} \tfrac{1}{2^{2\alpha}} [D^{(2\alpha,0)} f(0, t_2) p_\alpha(1-2t_1) + D^{(2\alpha,0)} f(\tfrac{1}{2}, t_2) p_\alpha(2t_1)] \\ & + \sum_{\beta=0}^{n} \tfrac{1}{2^{2\beta}} [D^{(0,2\beta)} f(t_1, 0) p_\beta(1-2t_2) + D^{(0,2\beta)} f(t_1, \tfrac{1}{2}) p_\beta(2t_2)]. \end{aligned} \tag{12}$$

Theorem 1. *Let $f \in C^l([0, \frac{1}{2}]^2)$. Then, the following decomposition formula holds:*

$$f(\mathbf{t}) = \tau_2(\mathbf{t}) - \tau_1(\mathbf{t}) + r(\mathbf{t}) \qquad (\mathbf{t} \in [0, \frac{1}{2}]^2), \tag{13}$$

and $r(\mathbf{t})$ can be extended into a 1-periodic odd function $\widetilde{r}(\mathbf{t})$ and $\widetilde{r} \in C^l(\mathbb{R}^2)$.

Proof. By (9), we know that $D^{(2\mu)}p_\alpha(1) = \delta_{\alpha,\mu}$ and $D^{(2\mu)}p_\alpha(0) = 0$. Again, by (11), for $0 \le \mu, \nu \le n$,

$$D^{(2\mu,2\nu)}(\tau_1(0,t_2)) = \sum_{\beta=0}^{n} [\, D^{(2\mu,2\beta)}f(0,0)D^{(2\nu)}p_\beta(1-2t_2) + D^{(2\mu,2\beta)}f(0,\frac{1}{2})D^{(2\nu)}p_\beta(2t_2)\,].$$

By (12), we deduce that for $0 \le \mu, \nu \le n$ and $0 \le t_2 \le \frac{1}{2}$,

$$D^{(2\mu,2\nu)}(\tau_2(0,t_2)) = D^{(2\mu,2\nu)}f(0,t_2) + \sum_{\beta=0}^{n} [\, D^{(2\mu,2\beta)}f(0,0)D^{(2\nu)}p_\beta(1-2t_2) + D^{(2\mu,2\beta)}f(0,\frac{1}{2})D^{(2\nu)}p_\beta(2t_2)\,].$$

Therefore, for $0 \le \mu, \nu \le n$,

$$D^{(2\mu,2\nu)}(\tau_2(0,t_2) - \tau_1(0,t_2)) = D^{(2\mu,2\nu)}f(0,t_2) \qquad (0 \le t_2 \le \frac{1}{2}).$$

By (13), for $0 \le \mu, \nu \le n$,

$$D^{(2\mu,2\nu)}r(0,t_2) = 0 \qquad (0 \le t_2 \le \frac{1}{2}).$$

Similarly, we can deduce that for $0 \le \mu, \nu \le n$,

$$D^{(2\mu,2\nu)}r(\tfrac{1}{2},t_2) = 0 \qquad (0 \le t_2 \le \tfrac{1}{2}),$$
$$D^{(2\mu,2\nu)}r(t_1,0) = D^{(2\mu,2\nu)}r(t_1,\tfrac{1}{2}) = 0 \quad (0 \le t_1 \le \tfrac{1}{2}).$$

Finally

$$D^{(2\mu,2\nu)}r(\mathbf{t}) = 0 \qquad (\mathbf{t} \in tial([0,\frac{1}{2}]^2),\ 0 \le \mu, \nu \le n). \tag{14}$$

For r, an odd extension is performed, denoted by r^o,

$$r^o(t_1,t_2) = r(t_1,t_2) \quad (\mathbf{t} \in [0,\tfrac{1}{2}]^2),$$
$$r^o(-t_1,t_2) = r^o(t_1,-t_2) = -r^o(t_1,t_2) \quad (\mathbf{t} \in [-\tfrac{1}{2},\tfrac{1}{2}]^2).$$

From this and (14), it follows that $r^o \in C^{(l)}([-\frac{1}{2},\frac{1}{2}]^2)$. Again, a periodic extension is performed, denoted by $\widetilde{r}$,

$$\widetilde{r}(\mathbf{t}+\mathbf{m}) = r^o(\mathbf{t}) \quad (\mathbf{t} \in [-\frac{1}{2},\frac{1}{2}]^2,\ \mathbf{m} \in \mathbb{Z}^2),$$

so $\widetilde{r}$ is a 1-periodic odd function and $\widetilde{r} \in C^l(\mathbb{R}^2)$, and it can be reconstructed well using its two-dimensional periodic wavelet coefficients. □

By (4), the periodic wavelet coefficients of $\widetilde{r}$ decay as fast as $O(2^{-m(l+1)})$. Compared with this, if we directly compute traditional (periodic) wavelet coefficients of $f \in C^l([0,\frac{1}{2}]^2)$, due to discontinuity on the boundary, the obtained (periodic) wavelet coefficients decay as fast as $O(2^{-m})$.

By (12), $\tau_2(\mathbf{t})$ is determined by four derivative functions of f on the boundary of $[0,\frac{1}{2}]^2$:

$$\{D^{(2\alpha,0)}f(0,t_2)\}_{\alpha=0,1\dots,n}, \qquad \{D^{(2\alpha,0)}f(\frac{1}{2},t_2)\}_{\alpha=0,1,\dots,n},$$
$$\{D^{(0,2\beta)}f(t_1,0)\}_{\beta=0,1,\dots,n}, \qquad \{D^{(0,2\beta)}f(t_1,\frac{1}{2})\}_{\beta=0,1,\dots,n}.$$

Similarly to the above process, these four functions can be decomposed as

$$\begin{aligned}
D^{(2\alpha,0)}f(0,t_2) &= \sum_{\beta=0}^{n} \tfrac{1}{2^{2\beta}}\big(\, D^{(2\alpha,2\beta)}f(0,0)p_\beta(1-2t_2) + D^{(2\alpha,2\beta)}f(0,\tfrac{1}{2})p_\beta(2t_2)\,\big) + u_\alpha(t_2),\\
D^{(2\alpha,0)}f(\tfrac{1}{2},t_2) &= \sum_{\beta=0}^{n} \tfrac{1}{2^{2\beta}}\big(\, D^{(2\alpha,2\beta)}f(\tfrac{1}{2},0)p_\beta(1-2t_2) + D^{(2\alpha,2\beta)}f(\tfrac{1}{2},\tfrac{1}{2})p_\beta(2t_2)\,\big) + v_\alpha(t_2),\\
D^{(0,2\beta)}f(t_1,0) &= \sum_{\alpha=0}^{n} \tfrac{1}{2^{2\alpha}}\big(\, D^{(2\alpha,2\beta)}f(0,0)p_\alpha(1-2t_1) + D^{(2\alpha,2\beta)}f(\tfrac{1}{2},0)p_\alpha(2t_1)\big) + w_\beta(t_1),\\
D^{(0,2\beta)}f(t_1,\tfrac{1}{2}) &= \sum_{\alpha=0}^{n} \tfrac{1}{2^{2\alpha}}\big(\, D^{(2\alpha,2\beta)}f(0,\tfrac{1}{2})p_\alpha(1-2t_1) + D^{(2\alpha,2\beta)}f(\tfrac{1}{2},\tfrac{1}{2})p_\alpha(2t_1)\,\big) + \gamma_\beta(t_1).
\end{aligned} \tag{15}$$

From this, we have

$$\begin{aligned}
&u_\alpha^{(2\beta)}(0) = u_\alpha^{(2\beta)}(\tfrac{1}{2}) = 0, \quad v_\alpha^{(2\beta)}(0) = v_\alpha^{(2\beta)}(\tfrac{1}{2}) = 0,\\
&w_\beta^{(2\alpha)}(0) = w_\beta^{(2\alpha)}(\tfrac{1}{2}) = 0, \quad \gamma_\beta^{(2\alpha)}(0) = \gamma_\beta^{(2\alpha)}(\tfrac{1}{2}) = 0 \quad (\alpha,\beta = 0,1,\dots,n).
\end{aligned}$$

After odd extensions and then 1-periodic extensions for u_α, v_α, w_β and γ_β, we obtain four 1-periodic smooth odd functions u_α^*, v_α^*, w_β^*, $\gamma_\beta^* \in C^l(\mathbb{R})$. Similarly to the argument in (4), the one-dimensional periodic wavelet coefficients of these four periodic functions decay as fast as $O(2^{-m(l+1)})$. So, $\tau_2(\mathbf{t})$ can be reconstructed well using the value of the derivative of f on the four vertices of $[0,\frac{1}{2}]^2$ and the one-dimensional periodic wavelet coefficients. By (11), $\tau_1(\mathbf{t})$ can be reconstructed using the value of the derivative of f on the four vertices of $[0,\frac{1}{2}]^2$. Therefore, f can be reconstructed well using the value of the derivative of f on the four vertices of $[0,\frac{1}{2}]^2$ and the one-dimensional and two-dimensional fast-decaying periodic wavelet coefficients.

4. Our Improvement of the DWT: Full Version

In this section, the traditional DWT/DPWT is improved so that the impacts of the data boundary on the wavelet coefficients can be mitigated well. The full version of our improved algorithm is stated as follows.

For $f \in C^l([0,\frac{1}{2}]^2)$, assume that the sampling of f on $[0,\frac{1}{2}]^2$ is given by the following:

$$x_{n_1,n_2} = f\Big(\frac{n_1}{2^J}, \frac{n_2}{2^J}\Big)\;(n_1,n_2 = 0,1,\dots,2^{J-1}).$$

The derivatives on the boundary of the square are denoted by

$$x_{n_1,n_2}^{(\alpha,\beta)} = D^{(2\alpha,2\beta)}f\Big(\frac{n_1}{2^J}, \frac{n_2}{2^J}\Big) \qquad (n_1 = 0, 2^{J-1} \text{ or } n_2 = 0, 2^{J-1};\ \alpha,\beta = 0,1,\dots,[l/2]). \tag{16}$$

Based on (11) and (12), we define $y_{n_1,n_2}^{(1)}$ and $y_{n_1,n_2}^{(2)}$ as

$$\begin{aligned}
y_{\mathbf{n}}^{(1)} = \tau_1(\tfrac{\mathbf{n}}{2^J}) = \sum_{\alpha,\beta=0}^{n} \tfrac{1}{2^{2\alpha+2\beta}}\big[&x_{0,0}^{(\alpha,\beta)}p_\alpha(1-\tfrac{2n_1}{2^J})p_\beta(1-\tfrac{2n_2}{2^J}) + x_{0,2^{J-1}}^{(\alpha,\beta)}p_\alpha(1-\tfrac{2n_1}{2^J})p_\beta(\tfrac{2n_2}{2^J})\\
&+x_{2^{J-1},0}^{(\alpha,\beta)}p_\alpha(\tfrac{2n_1}{2^J})p_\beta(1-\tfrac{2n_2}{2^J}) + x_{2^{J-1},2^{J-1}}^{(\alpha,\beta)}p_\alpha(\tfrac{2n_1}{2^J})p_\beta(\tfrac{2n_2}{2^J})\big]\\
&(\mathbf{n} = (n_1,n_2),\ n_1,n_2 = 0,1,\dots,2^{J-1}),
\end{aligned} \tag{17}$$

$$y^{(2)}_{\mathbf{n}} = \tau_2(\tfrac{\mathbf{n}}{2^J}) = \sum_{\alpha=0}^{n} \tfrac{1}{2^{2\alpha}}[x^{(\alpha,0)}_{0,n_2} p_\alpha(1-\tfrac{2n_1}{2^J}) + x^{(\alpha,0)}_{2^{J-1},n_2} p_\alpha(\tfrac{2n_1}{2^J})]$$
$$+ \sum_{\beta=0}^{n} \tfrac{1}{2^{2\beta}}[x^{(0,\beta)}_{n_1,0} p_\beta(1-\tfrac{2n_2}{2^J}) + x^{(0,\beta)}_{n_1,2^{J-1}} p_\beta(\tfrac{2n_2}{2^J})] \tag{18}$$
$$(\mathbf{n}=(n_1,n_2),\ n_1,n_2=0,1,\ldots,2^{J-1}).$$

The discrete data, x_{n_1,n_2}, can be decomposed as follows:

$$x_{n_1,n_2} = y^{(2)}_{n_1,n_2} - y^{(1)}_{n_1,n_2} + z_{n_1,n_2} \qquad (n_1,n_2=0,1,\ldots,2^{J-1}). \tag{19}$$

By (17)–(19), we have

$$z_{n_1,n_2} = 0, \qquad (n_1 = 0, 2^{J-1} \text{ or } n_2 = 0, 2^{J-1}).$$

An odd extension for the data $\{z_{n_1,n_2}\}$ is performed as follows:

$$z^o_{2^{J-1}+k,n_2} = -z_{2^{J-1}-k,n_2},\ z^o_{n_1,2^{J-1}+k} = -z^o_{n_1,2^{J-1}-k},\ z^o_{2^{J-1}+k,2^{J-1}+k} = z^o_{2^{J-1}-k,2^{J-1}-k} \tag{20}$$

where $n_1,n_2 = 0,1,\ldots,2^{J-1},\ k=1,\ldots,2^{J-1}-1$. Following this, the 2^J-periodic extension for $\{z^o_{n_1,n_2}\}$ is performed to obtain $\{z^*_{n_1,n_2}\}$.

Proposition 1. *For a large J, the periodic wavelet coefficients $c_{J,\mathbf{n}}$ of $\widetilde{r}$ satisfy*

$$c_{J,\mathbf{n}} \approx \frac{\lambda}{2^J} z^*_{\mathbf{n}} \qquad (n_1,n_2=0,1,\ldots,2^J-1),$$

where $\lambda = (\int_{\mathbb{R}} \varphi(t)dt)^2$ and $\widetilde{r}$ is stated in Theorem 1.

Proof. Comparing (13) and (19), it follows that $\{z^*_{n_1,n_2}\}$ is just the sampling of $\widetilde{r}$. Noticing that $\varphi^{per}_{0,J,\mathbf{n}}(\mathbf{t}) = \sum_{\mathbf{k}\in\mathbb{Z}^2} \varphi_{0,J,\mathbf{n}}(\mathbf{t}+\mathbf{k})$, by (2.6), it follows that

$$c_{J,\mathbf{n}} = \int_{[-\frac12,\frac12]^2} \widetilde{r}(\mathbf{t}) \sum_{\mathbf{k}\in\mathbb{Z}^2} \varphi_{0,J,\mathbf{n}}(\mathbf{t}+\mathbf{k})d\mathbf{t} = \sum_{\mathbf{k}\in\mathbb{Z}^2} \int_{[-\frac12,\frac12]^2+\mathbf{k}} \widetilde{r}(\mathbf{t})\varphi_{0,J,\mathbf{n}}(\mathbf{t})d\mathbf{t} = \int_{\mathbb{R}^2} \widetilde{r}(\mathbf{t})\varphi_{0,J,\mathbf{n}}(\mathbf{t})d\mathbf{t}.$$

Denote the compact support of φ_0 by Ω. Noticing that $\varphi_{0,J,\mathbf{n}}(\mathbf{t}) = 2^J\varphi_0(2^J\mathbf{t}-\mathbf{n})$ and $\widetilde{r} \in C^l(\mathbb{R}^2)$, we have

$$\begin{aligned}
c_{J,\mathbf{n}} &= 2^J \textstyle\int_{\mathbb{R}^2} \widetilde{r}(\mathbf{t})\varphi_0(2^J\mathbf{t}-\mathbf{n})d\mathbf{t} = 2^{-J}\int_{\mathbb{R}^2} \widetilde{r}(2^{-J}\mathbf{u})\varphi_0(\mathbf{u}-\mathbf{n})d\mathbf{u} \\
&= 2^{-J} \textstyle\int_{\mathbb{R}^2} \widetilde{r}(2^{-J}(\mathbf{u}+\mathbf{n}))\varphi_0(\mathbf{u})d\mathbf{u} = 2^{-J}\int_{\Omega} \widetilde{r}(2^{-J}(\mathbf{u}+\mathbf{n}))\varphi_0(\mathbf{u})d\mathbf{u} \\
&= 2^{-J}\big(\widetilde{r}(2^{-J}\mathbf{n}) \textstyle\int_{\mathbb{R}^2} \varphi_0(\mathbf{u})d\mathbf{u} + \int_{\Omega}(\widetilde{r}(2^{-J}(\mathbf{u}+\mathbf{n})) - \widetilde{r}(2^{-J}\mathbf{n}))\varphi_0(\mathbf{u})d\mathbf{u}\big) \\
&= 2^{-J}(\lambda\widetilde{r}(2^{-J}\mathbf{n}) + O(2^{-J})),
\end{aligned}$$

i.e.,

$$c_{J,\mathbf{n}} \approx \frac{\lambda}{2^J}\widetilde{r}(2^{-J}\mathbf{n}) = \frac{\lambda}{2^J} z^*_{\mathbf{n}} \qquad (n_1,n_2=0,1,\ldots,2^{J-1}),$$

where

$$\lambda = \int_{\mathbb{R}^2} \varphi_0(\mathbf{u})d\mathbf{u} = \int_{\mathbb{R}^2} \varphi_0(u_1,u_2)du_1du_2 = \int_{\mathbb{R}^2} \varphi(u_1)\varphi(u_2)du_1du_2 = \left(\int_{\mathbb{R}} \varphi(t)dt\right)^2.$$

□

The wavelet coefficients $\{c_{J,\mathbf{n}}\}$ $(\mathbf{n}=(n_1,n_2),\ n_1,n_2=0,1,\ldots,2^J-1)$ can be decomposed as

$$\{c_{m_0,k_1,k_2}\}_{k_1,k_2=0,1,\ldots,2^{m_0}-1}, \qquad \{d_{\mu,m,k_1,k_2}\}_{\mu=1,2,3,k_1,k_2=0,1,\ldots,2^m-1,\, m=m_0,m_0+1,\ldots,J-1}. \tag{21}$$

Theorem 2. *Suppose that φ and $\widetilde{\varphi}$ are symmetric at $t=0$ and ψ and $\widetilde{\psi}$ are symmetric at $t=\frac{1}{2}$ and $t=-\frac{1}{2}$, respectively. Then periodic wavelet coefficients in (21) are symmetric:*

$$\begin{aligned}
&c_{m,2^m-k_1,k_2} = -c_{m,k_1,k_2}, && c_{m,k_1,2^m-k_2} = -c_{m,k_1,k_2},\\
&d_{1,m,2^m-k_1,k_2} = -d_{1,m,k_1,k_2}, && d_{1,m,k_1,2^m-k_2-1} = -d_{1,m,k_1,k_2},\\
&d_{2,m,2^m-k_1-1,k_2} = -d_{2,m,k_1,k_2}, && d_{2,m,k_1,2^m-k_2} = -d_{2,m,k_1,k_2},\\
&d_{3,m,2^m-k_1-1,k_2} = -d_{3,m,k_1,k_2}, && d_{3,m,k_1,2^m-k_2-1} = -d_{3,m,k_1,k_2}.
\end{aligned}$$

Proof. Since φ and $\widetilde{\varphi}$ are symmetric at $t=0$ and ψ and $\widetilde{\psi}$ are symmetric at $t=\frac{1}{2}$ and $t=-\frac{1}{2}$, respectively, by (6), it follows that

$$h^*_{-n} = h^*_n, \qquad \tau^*_{1+n} = \tau^*_{1-n}.$$

Based on the DPWT algorithm, by (20), we easily obtain the symmetry property of the wavelet coefficients. □

In (18), $\{y^{(2)}_{\mathbf{n}}\}$ is determined by four sequences $\{x^{(\alpha,0)}_{0,n_2}\}$, $\{x^{(\alpha,0)}_{2^J-1,n_2}\}$, $\{x^{(0,\beta)}_{n_1,0}\}$ and $\{x^{(0,\beta)}_{n_1,2^J-1}\}$, which can be decomposed further as follows:

$$\begin{aligned}
x^{(\alpha,0)}_{0,n_2} &= \sum_{\beta=0}^{n} \tfrac{1}{2^{2\beta}}\big(\, x^{(\alpha,\beta)}_{0,0}\, p_\beta(1-\tfrac{2n_2}{2^J}) + x^{(\alpha,\beta)}_{0,2^J-1}\, p_\beta(\tfrac{2n_2}{2^J})\,\big) + u_{\alpha,n_2},\\
x^{(\alpha,0)}_{2^J-1,n_2} &= \sum_{\beta=0}^{n} \tfrac{1}{2^{2\beta}}\big(\, x^{(\alpha,\beta)}_{2^J-1,0}\, p_\beta(1-\tfrac{2n_2}{2^J}) + x^{(\alpha,\beta)}_{2^J-1,2^J-1}\, p_\beta(\tfrac{2n_2}{2^J})\,\big) + v_{\alpha,n_2},\\
x^{(0,\beta)}_{n_1,0} &= \sum_{\alpha=0}^{n} \tfrac{1}{2^{2\alpha}}\big(\, x^{(\alpha,\beta)}_{0,0}\, p_\alpha(1-\tfrac{2n_1}{2^J}) + x^{(\alpha,\beta)}_{2^J-1,0}\, p_\alpha(\tfrac{2n_1}{2^J})\big) + w_{\beta,n_1},\\
x^{(0,\beta)}_{n_1,2^J-1} &= \sum_{\alpha=0}^{n} \tfrac{1}{2^{2\alpha}}\big(\, x^{(\alpha,\beta)}_{0,2^J-1}\, p_\alpha(1-\tfrac{2n_1}{2^J}) + x^{(\alpha,\beta)}_{2^J-1,2^J-1}\, p_\alpha(\tfrac{2n_1}{2^J})\,\big) + \gamma_{\beta,n_1}.
\end{aligned} \tag{22}$$

After odd extensions and then 1-periodic extensions for u_{α,n_2}, v_{α,n_2}, w_{β,n_1}, γ_{β,n_1}, we obtain four 2^J-periodic smooth sequences u^*_{α,n_2}, v^*_{α,n_2}, w^*_{β,n_1}, γ^*_{β,n_1}. Again, by (5), we obtain one-dimensional periodic wavelet coefficients of u^*_{α,n_2}, v^*_{α,n_2}, w^*_{β,n_1}, γ^*_{β,n_1}:

$$\begin{aligned}
&\{c^u_{m_0,k}\}_{k=0,1,\ldots,2^{m_0}-1}, && \{d^u_{m,k}\}_{k=0,1,\ldots,2^m-1,\, m=m_0,m_0+1,\ldots,J-1}.\\
&\{c^v_{m_0,k}\}_{k=0,1,\ldots,2^{m_0}-1}, && \{d^v_{m,k}\}_{k=0,1,\ldots,2^m-1,\, m=m_0,m_0+1,\ldots,J-1}.\\
&\{c^w_{m_0,k}\}_{k=0,1,\ldots,2^{m_0}-1}, && \{d^w_{m,k}\}_{k=0,1,\ldots,2^m-1,\, m=m_0,m_0+1,\ldots,J-1}.\\
&\{c^\gamma_{m_0,k}\}_{k=0,1,\ldots,2^{m_0}-1}, && \{d^\gamma_{m,k}\}_{k=0,1,\ldots,2^m-1,\, m=m_0,m_0+1,\ldots,J-1}.
\end{aligned} \tag{23}$$

Similar to Theorem 2, the above periodic wavelet coefficients are also symmetric.

Finally, we summarize our improvement of the discrete (periodic) wavelet transform for $\{x_{n_1,n_2}\}_{n_1,n_2=0,1,\ldots,2^J-1}$, as follows:

Decomposition Algorithm

Step 1. By (17)–(19), we obtain $\{z_{n_1,n_2}\}_{n_1,n_2=0,1,\ldots,2^J-1}$. After that, an odd extension and a periodic extension are performed for $\{z_{n_1,n_2}\}_{n_1,n_2=0,1,\ldots,2^J-1}$ to obtain $\{z^*_{n_1,n_2}\}_{n_1,n_2\in\mathbb{Z}^2}$. Finally, by Proposition 1 and (6), two-dimensional periodic wavelet coefficients are computed in (21). Again, by Theorem 2, the number of nonzero two-dimensional periodic wavelet coefficients that is necessary to store is $(2^{J-1}-1)^2$.

Step 2. By (22), u_{α,n_2}, v_{α,n_2}, w_{β,n_1}, γ_{β,n_1} can be obtained. After odd extensions, and then periodic extensions, we obtain four 2^J-periodic smooth sequences u^*_{α,n_2}, v^*_{α,n_2}, w^*_{β,n_1}, γ^*_{β,n_1}. Again, by (5), one-dimensional periodic wavelet coefficients are obtained as those in (23). Similar to Theorem 2, due to the symmetric property of periodic wavelet coefficients, the number of nonzero two-dimensional periodic wavelet coefficients that is necessary to store is $4 \times (2^{J-1} - 1)$.

Step 3. The following $4(n+1)^2$ values are stored:

$$\{x^{(\alpha,\beta)}_{0,0}\}, \quad \{x^{(\alpha,\beta)}_{0,2^{J-1}}\}, \quad \{x^{(\alpha,\beta)}_{2^{J-1},0}\}, \quad \{x^{(\alpha,\beta)}_{2^{J-1},2^{J-1}}\} \qquad (\alpha, \beta = 0, 1, \dots, n).$$

Reconstruction Algorithm.

Step 1. By (17), using the $4(n+1)^2$ values,

$$\{x^{(\alpha,\beta)}_{0,0}\}, \quad \{x^{(\alpha,\beta)}_{0,2^{J-1}}\}, \quad \{x^{(\alpha,\beta)}_{2^{J-1},0}\}, \quad \{x^{(\alpha,\beta)}_{2^{J-1},2^{J-1}}\} \qquad (\alpha, \beta = 0, 1, \dots, n),$$

we obtain $\{y^{(1)}_{n_1,n_2}\}_{n_1,n_2=0,1,\dots,2^{J-1}}$.

Step 2. Using the $4(n+1)^2$ values in Step 1, (22), (23) and the one-dimensional inverse discrete periodic wavelet transform, we obtain

$$\{x^{(\alpha,0)}_{0,n_2}\}, \quad \{x^{(\alpha,0)}_{2^{J-1},n_2}\} \quad (n_2 = 0, 1, \dots, 2^{J-1},\ \alpha = 0, 1, \dots, n)$$

$$\{x^{(0,\beta)}_{n_1,0}\}, \quad \{x^{(0,\beta)}_{n_1,2^{J-1}}\} \quad (n_1 = 0, 1, \dots, 2^{J-1},\ \beta = 0, 1, \dots, n),$$

and, by (18), we obtain $\{y^{(2)}_{n_1,n_2}\}_{n_1,n_2=0,1,\dots,2^{J-1}}$.

Step 3. By (21) and the two-dimensional inverse discrete periodic wavelet transform, we obtain $\{z^*_{n_1,n_2}\}$. This means that $\{z_{n_1,n_2}\}_{n_1,n_2=0,1,\dots,2^{J-1}}$ can be computed.

Step 4. By (17), we can reconstruct f:

$$x_{n_1,n_2} = y^{(2)}_{n_1,n_2} - y^{(1)}_{n_1,n_2} + z_{n_1,n_2} \qquad (n_1, n_2 = 0, 1, \dots, 2^{J-1}).$$

5. Numerical Experiments

We compared our improved DWT with the classic DWT through numerical experiments. The quality of data approximation was measured by the known peak signal-to-noise ratio (PSNR) [17]:

$$\mathrm{PSNR} = 20 \log_{10} \left\{ \frac{\max\limits_{m,n} |x_{m,n}|}{\mathrm{RMSE}} \right\},$$

where $\{x_{m,n}\}$ is the original data, RMSE is the mean squared error between the original and the approximation divided by the square root of the total number of samples.

For the discrete data $x_{m,n} = e^{\frac{m}{128} + \frac{n}{128}}$ $(m, n = 0, 1, 2, \dots, 127)$, we used the simplest version of our algorithm, which meant that no numerical derivative was computed to approximate $\{x_{m,n}\}$. In the approximation and reconstruction processes, we retained a certain number of the largest coefficients in terms of energy from all one/two-dimensional wavelet coefficients and then reconstructed the original data from them. Figure 1 shows the quality of the approximations by using DWT and our improvement, where the depth of wavelet decomposition was set to the maximum level. The higher value of the PSNR indicated a better approximation performance. It was clear that the simplified version of our algorithm had a better approximation performance than that of the classic DWT. Noticing that the PSNR value is in terms of logarithmic scale, the smaller the number of retained coefficients, the clearer the performance difference became.

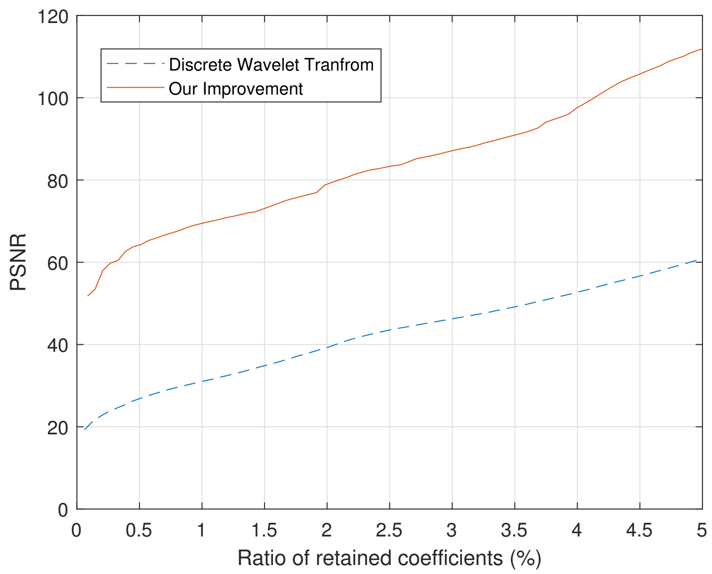

Figure 1. Approximation quality of the discrete wavelet transform and our improved algorithm.

6. Discussion and Conclusions

The discrete wavelet transform and the discrete periodic wavelet transform is widely used in signal processing, data compression and wireless communication. Due to discontinuity on the boundary of the original data, the decay rate of the obtained wavelet coefficients was slow. In this study, we introduced a combination of polynomial interpolation and one-dimensional/two-dimensional discrete periodic wavelet transforms to mitigate these boundary effects. Due to the smooth extension in our algorithm, the one-dimensional and two-dimensional periodic wavelet coefficients in our algorithm decayed as fast as $O(2^{-m(l+1)})$. Compared with this, if we applied the traditional discrete (periodic) wavelet transform, due to discontinuity on the boundary, the corresponding wavelet coefficients decayed as fast as $O(2^{-m})$. Even if we considered the simplest version of our algorithm (i.e., taking $n = 0$ in (17) and (18), which meant that no numerical derivative was computed), the corresponding wavelet coefficients in our algorithm still decayed as fast as $O(2^{-3m})$, which was faster than that of the traditional discrete (periodic) wavelet transform (i.e., $O(2^{-m})$). Moreover, the numerical experiment also demonstrated that the simplest version of our algorithm could compress the data much better than the traditional discrete wavelet transform. The full version of our algorithm could be applied to compress smoother data, e.g., CMIP6 data [13]. The size of CMIP6 data increases sharply at the petabyte scale [19], but, even now, there is still no good algorithm to compress it. Since CMIP6 data are output data from numerical solutions of fluid equations and energy equations governing the Earth's climate system [18], CMIP6 data is smooth and the derivative values on the data boundary are easily estimated, so our algorithm could compress this kind of data well.

Funding: This research was partially supported by European Commissions Horizon 2020 Framework Program No. 861584 and Taishan Distinguished Professor Fund.

Data Availability Statement: Not applicable.

Acknowledgments: The author thanks the reviewers and editors for their valuable comments.

Conflicts of Interest: The author declare no conflict of interest.

References

1. Mallat, S. *A Wavelet Tour of Signal Processing*; Academic Press: Cambridge, MA, USA, 2008.
2. Zhang, Z.; Jorgenson, P.E.T. *Frame Theory in Data Science*; Springer: Heidelberg, Germany, 2021.

3. Jha, C.K.; Kolekar, M.H. Tunable Q-wavelet based ECG data compression with validation using cardiac arrhythmia patterns. *Biomed. Signal Process. Control* **2021**, *66*, 102464.
4. Otsuka, A.; Muramatsu, K.; Nagata, F. Data-driven generation of random skin model shapes by using wavelet transformation. *Comput. Ind. Eng.* **2020**, *150*, 106860. [CrossRef]
5. Chakraborty, J.; Nandy, A. Discrete wavelet transform based data representation in deep neural network for gait abnormality detection. *Biomed. Signal Process. Control* **2020**, *62*, 102076. [CrossRef]
6. Kamgar, R.; Dadkhah, M.; Naderpour, H. Seismic response evaluation of structures using discrete wavelet transform through linear analysis. *Structures* **2021**, *29*, 863–882. [CrossRef]
7. Deriaz, E.; Farge, M.; Schneider, K. Craya decomposition using compactly supported biorthogonal wavelets. *Appl. Comput. Harmon. Anal.* **2010**, *28*, 267–284. [CrossRef]
8. Chen, Q.; Cao, H.; Shi, Z. Construction and decomposition of biorthogonal vector-valued wavelets with compact support Chaos. *Solitons Fractals* **2009**, *42*, 2765–2778. [CrossRef]
9. Antolin, A.S.; Zalik, R.A. Compactly supported Parseval framelets with symmetry associated to E(2)d(Z) matrices. *Appl. Math. Comput.* **2018**, *325*, 179–190. [CrossRef]
10. Atreasa, N.; Karantzasb, N.; Papadakisb, M.; Stavropoulosc, T. On the design of multi-dimensional compactly supported Parseval framelets with directional characteristics. *Linear Algebra Appl.* **2019**, *582*, 1C36.
11. Dutkay, D.E.; Jorgensen, P.E.T.; Silvestrov, S. Decomposition of wavelet representations and Martin. *J. Funct. Anal.* **2012**, *262*, 1043–1061. [CrossRef]
12. Averbuch, A.Z.; Neittaanmäki, P.; Zheludev, V.A. *Spline and Spline Wavelet Methods with Applications to Signal and Image Processing*; Springer: Berlin/Heidelberg, Germany, 2016. [CrossRef]
13. Zeng, C.; Lai, W.; Lin, H.; Liu, G.; Qin, B.; Kang, Q.; Feng, X.; Yu, Y.; Gu, R.; Wu, J.; et al. Weak information extraction of gamma spectrum based on a two-dimensional wavelet transform. *Radiat. Phys. Chem.* **2023**, *208*, 110914.
14. Alaifari, R.; Bartolucci, F.; Wellershoff, M. Phase retrieval of bandlimited functions for the wavelet transform. *Appl. Comput. Harmon. Anal.* **2023**, *64*, 102–117. [CrossRef]
15. Lin, J.; Zhou, W.; Cui, X.Z.; Hong, H.P. Application of wavelet transforms to the simulation of corrosion fields on buried pipelines. *Comput. Struct.* **2023**, *276*, 106957. [CrossRef]
16. Torrence, C.; Compo, G.P. A practical guide to wavelet anal- ysis. *Bull. Am. Meteorol. Soc.* **1998**, *79*, 61–78. [CrossRef]
17. Najmi, A.; Moon, T. *Advanced Signal Processing*; McGraw-Hill: New York, NY, USA, 2020. [CrossRef]
18. Eyring, V.; Bony, S.; Meehl, G.A.; Senior, C.A.; Stevens, B.; Stouffer, R.J.; Taylor, K.E. Overview of the Coupled Model Intercomparison Project Phase 6 (CMIP6) experimental design and organization. *Geosci. Model Dev.* **2016**, *9*, 1937–1958.
19. Reichstein, M.; Camps-Valls, G.; Stevens, B.; Jung, M.; Denzler, J.; Carvalhais, N. Deep learning and process understanding for data-driven Earth system science. *Nature* **2019**, *566*, 195C204. [CrossRef]